Article

Tunable Electromagnetically Induced Transparent Window of Terahertz Metamaterials and Its Sensing Performance

Zhenlin Wu [1], Peiyao An [1], Menghan Ding [1], Yanan Qi [1], Lin Zhang [1], Shaoshuai Han [1], Di Lian [1], Changming Chen [2] and Xin Yang [3,*]

[1] School of Optoelectronic Engineering and Instrumentation Science, Dalian University of Technology, Dalian 116024, China; zhenlinwu@dlut.edu.cn (Z.W.); anpeiyao@mail.dlut.edu.cn (P.A.); dingmenghan@mail.dlut.edu.cn (M.D.); qiyanan_crystal@mail.dlut.edu.cn (Y.Q.); zhanglin1998@mail.dlut.edu.cn (L.Z.); 779102711@mail.dlut.edu.cn (S.H.); liandi@mail.dlut.edu.cn (D.L.)

[2] State Key Laboratory of Optoelectronic Integration, College Electronic Science & Engineering, Jilin University, Changchun 130012, China; chencm@jlu.edu.cn

[3] Department of Electrical and Electronics Engineering, School of Engineering, Cardiff University, Cardiff CF10 3AT, UK

[*] Correspondence: yangx26@cardiff.ac.uk; Tel.: +44-2920-875-708

Abstract: The electromagnetically induced transparency effect of terahertz metamaterials exhibits excellent modulation and sensing properties, and it is critical to investigate the modulation effect of the transparent window by optimizing structural parameters. In this work, a unilateral symmetrical metamaterial structure based on the cut-wire resonator and the U-shaped split ring resonator is demonstrated to achieve electromagnetically induced transparency-like (EIT-like) effect. Based on the symmetrical structure, by changing the structural parameters of the split ring, an asymmetric structure metamaterial is also studied to obtain better tuning and sensing characteristics. The parameters for controlling the transparent window of the metamaterial are investigated in both passive and active modulation modes. In addition, the metamaterial structure based on the cut-wire resonator, unilateral symmetric and asymmetric configurations are investigated for high performance refractive index sensing purposes, and it is found that the first two metamaterial structures can achieve sensitivity responses of 63.6 GHz/RIU and 84.4 GHz/RIU, respectively, while the asymmetric metamaterial is up to 102.3 GHz/RIU. The high sensitivity frequency response of the proposed metamaterial structures makes them good candidates for various chemical and biomedical sensing applications.

Keywords: terahertz; metamaterial; electromagnetically induced transparency-like effect; refractive index sensing

1. Introduction

Electromagnetically induced transparency effect is observed in atomic systems, which occurs due to quantum interference phase extinction effects. The EIT-like effect of metamaterials can provide a narrow-band transparent window under the background of broadband absorption [1]. EIT is usually accompanied by strong dispersion, which can significantly reduce the propagation group velocity of terahertz pulses [2]. This unique property makes it suitable for the fabrication of refractive index sensors [3], optical switches, optical modulators, optical filters, and slow light devices [4–6]. However, traditional EIT requires harsh conditions such as high temperature and high-intensity laser. Metamaterials are a kind of electromagnetic material with periodic cell array, which can be designed manually. Compared with natural materials and chemical synthetic materials, artificial metamaterials have attracted the attention of researchers due to their unique electromagnetic advantages, such as negative conductivity and negative permeability [7–9]. Many structures of EIT have been proposed, including cut wires resonators (CWR) [10], and split-ring resonators (SRR) [11,12]. Some other symmetric typical terahertz metamaterials structures, including

fishing net structure [13], dipole-coupled quadrupole [14] have also been investigated to achieve EIT-like phenomenon. For example, in 2008, Zhang et al. [15] found that plasma induced transparency (PIT) can be generated through the near-field coupling of "bright-mode" structure and "dark mode" structure, and demonstrated an EIT-like effect using electromagnetic metamaterials. In 2013, Zhu et al. [16] realized a broadband EIT-like effect by using a transverse tangent and four open resonant rings. In 2019, Wu et al. [17] realized the EIT-like effect by using SSRR and CSRR. Most research works focused on the design of the metamaterial structures and further analysis of coupling mechanism between each component of the metamaterial device. However, the transparent windows of these studies have been realized at a fixed frequency. It is essential to reconstruct the geometries or modify the substrates if the resonance needs to be tuned to different working frequencies.

In order to improve the sensor performance, many materials are adopted to construct EIT-like structures including graphene and 3D Dirac semimetals. The optical response of graphene can be dynamically adjusted by the Fermi energy or the coupling strength between the two layers. For example, Xia et al. [18] designed a PIT metamaterial structure, which is composed of a sinusoidally curved and a planar graphene layer. Shu et al. [19] proposed and simulated a novel tunable EIT in terahertz metal-graphene metamaterial. The amplitude of EIT window can be modulated by changing the Fermi level of graphene. Patel et al. [20] designed a double layer of gold multipattern swastika (DLMP) resonator based on SiO_2 substrate. Although graphene possesses outstanding optical properties, enabling dynamic control of electromagnetic waves, its coupling with light is not strong enough to enable it to be used directly in practice owing to its ultrathinness in space. The 3D Dirac semimetal is also called '3D graphene'. Shen et al. [21] proposed a complementary BDS metamaterial structure to achieve a tunable EIR effect with a high Q-factor. However, the dielectric constants of 3D Dirac semimetals are dynamically regulated mainly by changing their Fermi energy. For some 3D Dirac semimetals such as $PdTe_2$, $PdSe_2$, and $PtTe_2$, the Dirac point is far from the Fermi surface, which makes experimental modulation more difficult.

In some practical applications, it is very important to modulate the transparent window of the EIT-like phenomenon, which can realize terahertz modulators and the terahertz switches. By changing the material structures or varying the external parameters, two types of modulations can be achieved, i.e., passive modulation and active modulation. Firstly, passive modulation is generally achieved by changing the geometric parameters of the structure [22,23], but in each modulation the structure needs to be remanufactured, which becomes too complicated and confines its applications. Active modulation manifests as real-time adjustment of the transparent window. It can be operated by external fields such as temperature modulation, light modulation, or DC electric field modulation [10,17,24]. It is necessary to optimize the design of the metamaterial structure to achieve a better transparent window in the terahertz band and expand more novel application functions of terahertz metamaterials such as high sensitivity, high Q-factor, and tunable EIT-like effect.

So far, many applications of the EIT-like phenomenon are investigated based on the bright-dark modes coupling theory [25]. In this work, two symmetrical/asymmetric metamaterial structures based on cut-wire resonators and U-shaped split ring resonators have been proposed to realize the EIT-like window. The EIT-like effect of several metamaterials with different structures as well as the properties of modulation and sensing are studied. By analyzing the modulation characteristics of passive and active modulation, and simulating the refractive index sensing of both structures, the potential value of metamaterial structure in a terahertz switch and terahertz sensor have been investigated.

2. Design and Simulation

Firstly, a metamaterial structure was designed based on the combination of traditional Cut Wire (CW) resonator as bright mode and a pair of U-Shaped Split Ring (USR) resonator as dark mode. Two of the USRs were on the same side of CW and were symmetrically distributed up and down to form a unilateral symmetric structure, as shown in Figure 1a.

In order to achieve the EIT-like window at certain wavelength band, the software, CST Microwave Studio was used to calculate the electromagnetic field of metamaterial by optimizing various parameters, including the length of CW structure L, the width of CW w_1, two side lengths of USRs, a & b, as well as the width of USRs w_2. The period of metamaterial unit was set as $P_x = P_y = 120$ μm. Each base structure consisted of a substrate material as the lower layer and a metallic material with a special structure as the upper layer. The substrate was made of lossless quartz with a dielectric constant ε of 3.75 and a thickness of 20 μm was utilized. A 200 nm gold layer with a conductivity σ of 4.6×10^7 S/m was selected to better form the bright and dark mode to realize the EIT effect. The size parameters of L, a, b, w_1 and w_2, were set as 90 μm, 40 μm, 30 μm, 6 μm, and 4 μm, respectively, while the coupling distance δ_x and δ_y were fixed as 4 μm and 30 μm. For the design of the asymmetric metamaterial structure, the upper and lower USRs were asymmetrically distributed with respect to the transverse central axis, as shown in Figure 2a. The coupling distance δ_{xup} between the CW and the upper USR was set to be 13 μm, and the coupling distance δ_{xdown} between the CW and the lower USR was set to be 4 μm, other parameters remained unchanged as the symmetrical structure. The CST simulation used a frequency domain solver with a tetrahedral mesh, and the boundary conditions in the x and y axes both used the unit cell, while the z direction was set as open (add space) and the Floquet mode is set as 2. The incident terahertz wave was set to be vertical with respect to the surface of the metamaterial to explore the transmission characteristics of the EIT-like effect.

(a)

(b)

(c)
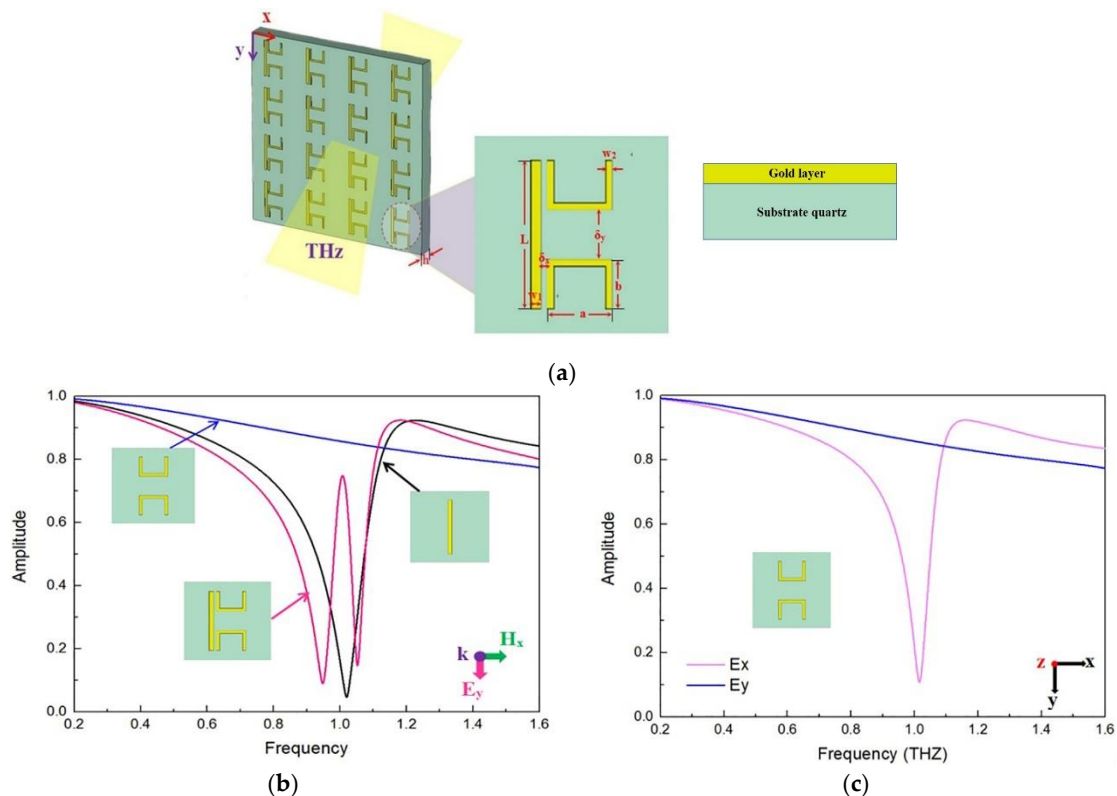
Figure 1. The transmission properties of metamaterials based on different symmetrical structures. (**a**) Schematic diagram of metamaterial structure; (**b**) The transmission spectra of CW (black), USRs (blue), and CW+USRs array (red) in the direction of E_y electric field. The CW resonator shows typical LSP resonance at 1.01 THz, while an electromagnetically induced transparency-like window can be found in the CW + USRs structure; (**c**) The transmission spectra of USR array in the direction of E_x and E_y electric fields, the horizontal orientation of the incident electric field can excite the LC resonance of USRs at similar frequencies.

(**a**)   (**b**)
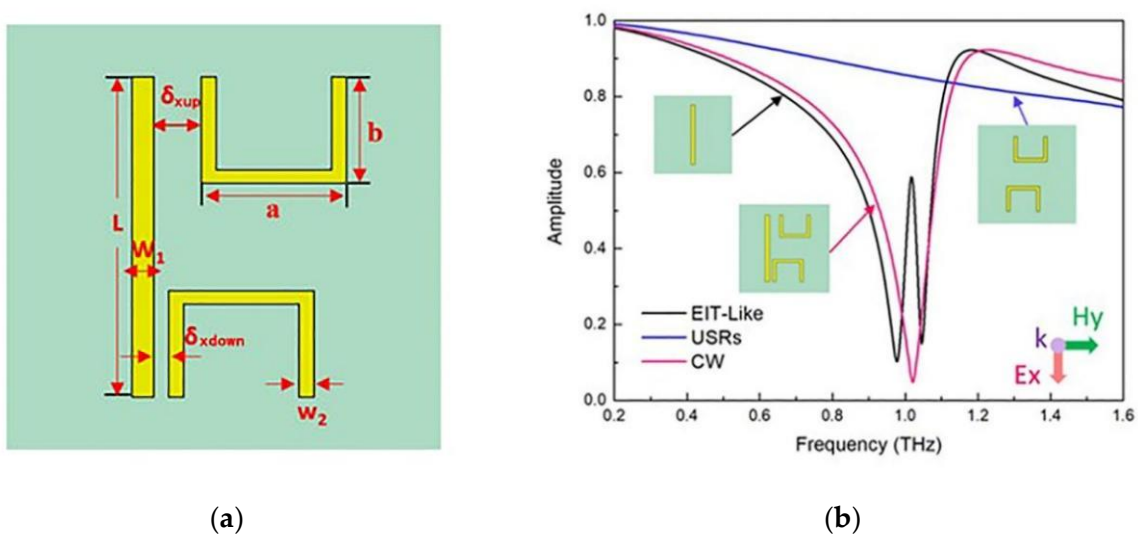
Figure 2. The transmission properties of metamaterial structure based on asymmetric structures. (**a**) Asymmetric structure distribution of upper and lower USRs with different distances from the CW; (**b**) The transmission spectra of the asymmetric EIT structure shows a transparent window similar as the symmetric structure at 1.02 THz.

Based on the designed symmetrical structure, three groups of metamaterials were analyzed. The first group of metamaterials consisted of CW resonator arrays only, the second group of metamaterials consisted of USRs array only, and the third group consisted of both the CW and USRs structures. The normalized transmission spectra of the three metamaterial groups are shown in Figure 1b. It can be seen that the CW resonator array shows a typical local surface plasmon resonance (LSP) at 1.01 THz, indicating that as the incident electric field is parallel to the CW, the electromagnetic radiation can be directly coupled into the CW; however, since the incident electric field is vertical, it becomes ineffective for USR excitation under the same frequencies. In Figure 1c, it can be found that the horizontal direction of the incident electric field can excite the LC resonance of USRs at similar frequencies. Therefore, CW and USRs can be used as the bright and dark modes of the vertical electric field excitation, satisfying the prerequisite conditions required to realize the bright-dark mode of the EIT-like effect. In the designed EIT structure, the CW was directly excited by the terahertz wave along the incident electric field to generate electrical resonance, and the near-field coupling simultaneously excited the LC resonance in the USRs. The destructive interference between LSP and LC resonance resulted in a clear transparent peak in a broad absorption background at 1.01 THz, showing an electromagnetically induced transparency-like window. In addition, the left and right transmission troughs were located at 0.95 THz and 1.05 THz, respectively. Moreover, the asymmetric structure was simulated and analyzed, while a transparent window could also be found, similar to the symmetric structure. The window was located at 1.02 THz, and the left and right transmission troughs were at 0.98 THz and 1.05 THz, respectively, see Figure 2b.

Based on the optimized parameters of metamaterial structure, the electromagnetic field of the symmetric structure metamaterial was simulated and analyzed, as shown in Figure 3. The electromagnetic field distribution (Figure 3a,b) and surface current distribution map (Figure 3c) of the three characteristic frequencies (0.95 THz, 1.01 THz, and 1.05 THz) were used to analyze the coupling of bright and dark modes. It was found that its coupling in the electromagnetic field was very weak at the transmission trough points of 0.95 THz and 1.05 THz. In addition, in the surface current distribution shown in Figure 3c, it can be noted that the surface current directions of CW and USRs at low-frequency trough are opposite, while the currents at high-frequency trough are in the same direction. By observing the transparent window at a frequency of 1.01 THz, it can be found that the bright mode is significantly suppressed while the dark mode is excited. This is because the bright mode

CW generates an asymmetrical distribution of electric field on both sides of USR after being radiated by the incident wave, and the x component of the electric field excites the LC resonance of USR, so that part of the energy of the bright mode is transferred to the dark mode. This is a typical phenomenon of interference between bright and dark resonators, which fully indicates that the structure we propose can achieve EIT-like effects. In addition, Figure 3d–f shows the electromagnetic field distribution at three frequencies corresponding to the asymmetric structure.
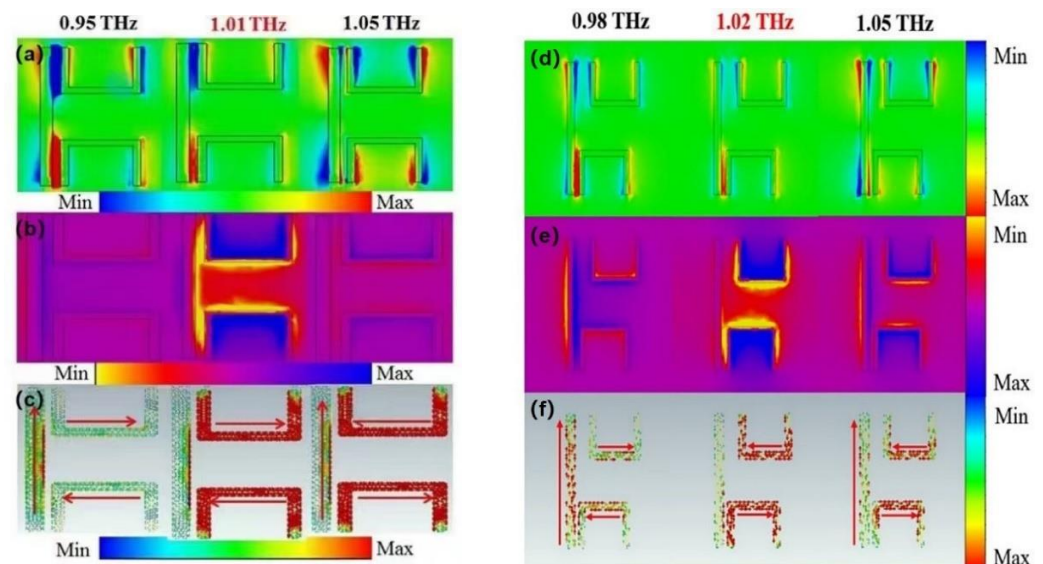

Figure 3. The distribution of electromagnetic field and surface current corresponding to three different characteristic frequencies. (**a**,**b**) The electromagnetic field distribution at frequencies of 0.95 THz, 1.01 THz, 1.05 THz, and the coupling between the bright and dark mode at troughs of 0.95 THz and 1.05 THz are very weak; (**c**) The surface current distribution of symmetrical structure at different frequencies (the red arrow indicates the current direction), the current directions at the low-frequency trough are opposite, while at high-frequency trough are in the same direction; (**d**–**f**) The electromagnetic field distribution of asymmetric structure at three characteristic frequencies.

3. Results and Discussion

3.1. Passive Modulation of Metamaterial EIT-like Window

The EIT-like effect is caused by the coupling and destructive interference between the bright and dark eigenmodes [26,27], when the coupling distance changes, the coupling strength will change accordingly, leading to the modulation of the EIT-like effect. The influence of the distance δ on the EIT window was investigated by varying the distance δ_x between CW and USRs in the symmetric structure and the distance δ_y between the upper and lower USRs. As shown in Figure 4a, the horizontal distance δ_x between the CW and USRs was varied from 1 μm to 17 μm with the distance fixed δ_y distance of 30 μm to show the influence of the modulation effect of the transparent window. It can be found that when δ_x is 1 μm and 5 μm, the electric field was mainly confined in the dark mode, which indicates that most of the energy of the bright mode CW had been coupled into the dark mode. As the relative distance δ_x between the bright and dark modes increased, the coupling between the eigenmodes became weaker. The two resonance troughs of LSP resonance and LC resonance decreased and drew closer at the same time, with the transparent window blue-shifted. When δ_x reached 17 μm, the coupling disappeared completely, and the transparency window disappeared, too. While the influence of vertical distance $\delta_y \neg$, δ_x was fixed as 4 μm, the transparent window could be modulated by changing the δ_y from 28 μm to 12 μm. It can be seen from Figure 4b that, when $\delta_y = 28$ μm, the incident THz wave and CW were strongly coupled, and the dark mode was also excited by near-field coupling. As a result, the electric field in the bright mode was suppressed,

therefore, a transparent window was found around 1 THz. As the USR pairs approached each other, the relative distance $\delta_y \neg$ decreased, the coupling between eigenmodes was weakened, while the LC resonance troughs gradually disappeared. When $\delta_y = 12$ μm, the induced magnetic fields caused by the surface currents of the two USR pairs suppressed each other, and the induced magnetic field regions were cancelled out, as a result, the dark mode could not be successfully excited, and the EIT-like window disappeared. Moreover, as seen from Figure 4, as δ_x increased, the transparent window became narrower, which can be attributed to the reduced coupling of the CW and the USRs resonator. In contrast, when δ_y was reduced from 28 μm to 20 μm, it was noticed that the influence was more of a frequency drift rather than changing the EIT window width. This behavior indicated that by changing the coupling between the bright and the dark modes, the EIT-like effect could be effectively modulated.

(**a**)   (**b**)
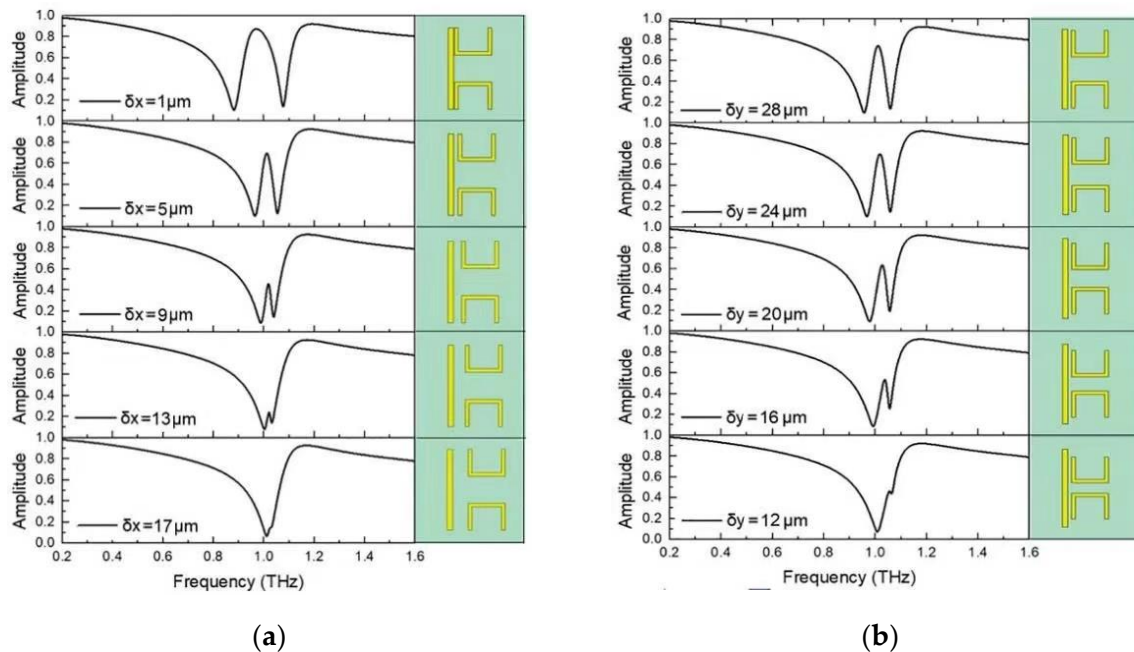
Figure 4. The influence of structural parameters on transmission characteristics. (**a**) The transmission spectra at various coupling distances between CW and USRs, as the δx increases, the two resonance troughs of LSP and LC decrease and get closer, with the transparent window blue-shifted; (**b**) The transmission spectra at various coupling distances between USR pairs, as the δy decreases, the LC resonance trough gradually disappears, while the transparent window also disappears.

For asymmetric structures, the horizontal position between the upper and lower asymmetric USRs were kept unchanged to investigate the influence of the distance δ_x between CW and asymmetric USRs and the distance δ_y between the upper and downer USRs on the EIT-like effects. As shown in Figure 5a, the horizontal distance δ_x was varied from 1 μm to 9 μm with fixed δ_y of 30 μm to show the influence of the modulation effect of the transparent window. It can be found that when δ_x was 1 μm, 3 μm, and 5 μm, the electric field was mainly confined in the dark mode. As the relative distance δ_x increased, the coupling between the eigenmodes became weaker. Two resonance troughs of LSP resonance and LC resonance decrease and drew closer to each other at the same time, together with the transparent window blue-shifted. As δ_x reached 9 μm, the coupling disappeared completely, and the transparency window disappeared, too. Compared with the symmetric distribution of dark modes, the width of the EIT-like window was narrower, while the coupling distance δ_x was smaller. Furthermore, for the influence of the vertical distance δ_y between the USR pairs on the transmission characteristics, δ_{xup} was fixed as 13 μm and $\delta_{xdown} = 4$ μm, the transparent window was modulated by varying δ_y from 28 μm to 12 μm. It can be seen from Figure 5b that when $\delta_y = 28$ μm, the incident THz

wave and CW were strongly coupled, and the dark mode was also excited by near-field coupling. As USRs approached each other, the distance δ_y decreased, so the coupling between bright and dark modes was weakened, while the LC resonance trough gradually disappeared. When δ_y = 12 μm, the EIT-like window disappeared. This is similar as that of the symmetric structure.

(**a**)   (**b**)
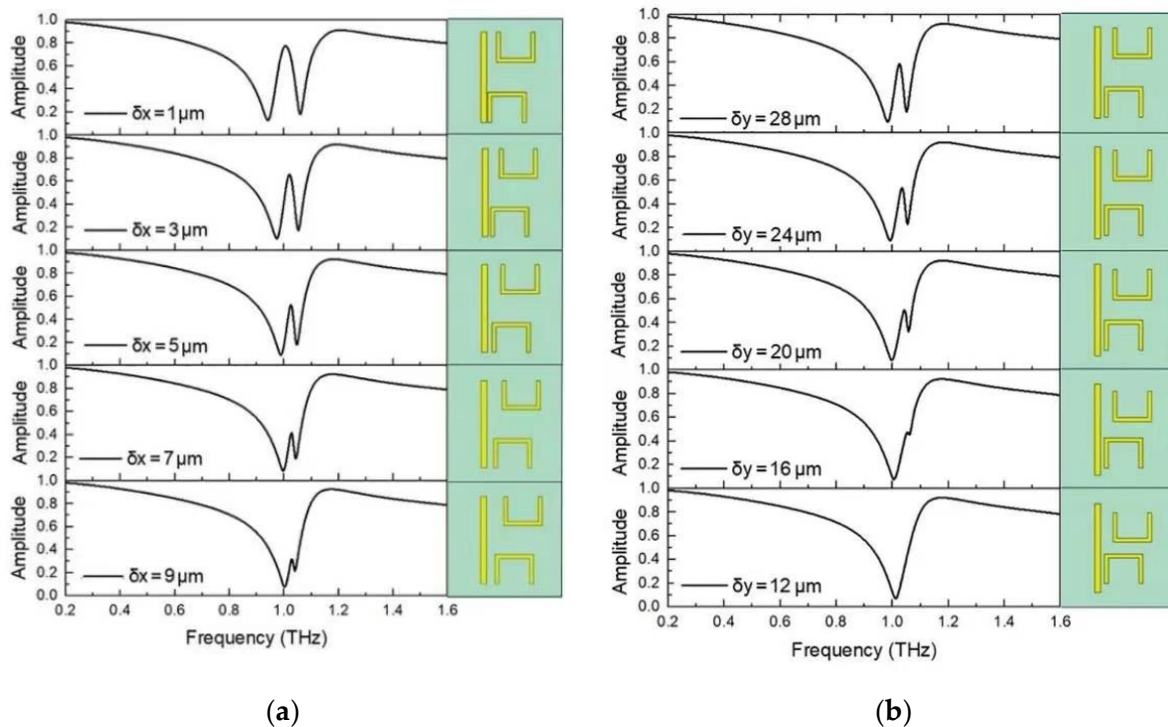
Figure 5. The influence of the asymmetric structural parameters on the transmission characteristics. (**a**) The transmission spectra with various coupling distances δ_x between CW and USRs, the coupling distance δx is smaller than that of the symmetric structure; (**b**) The transmission spectra with various coupling distances δ_y between USR pairs, similar to the symmetric structure.

3.2. Active Modulation of Metamaterial EIT-like Window

In the previous section, the modulation effect of parameter variation on transparent window was investigated under the passive modulation mode. However, under this mode, the parameters of the metamaterials were fixed, leading to a relatively high cost and limitations for practical uses. In this section, an active modulation method is proposed by introducing extra optical pumping to modulate transparent EIT-like window.

As the conductivity of photosensitive silicon (Si) can be changed by different incident light intensity, therefore, by introducing photosensitive Si at different locations of the metamaterial (between the bright and dark modes or between the two USRs), EIT-like windows can be modulated by simply varying the light intensity of the incident THz wave, which can be an effective and cheaper way of enhancing the tunability properties of the designed metamaterials.

As shown in Figure 6a,c, by burying photosensitive Si between bright and dark modes, an active modulation of the EIT-like effect could be achieved by changing the coupling effect between the eigenmodes. When there was no pumping, the conductivity of the photosensitive Si was very low, and the light and dark modes were electrically isolated. In this case, the induced current mainly flowed around the two USRs, as a result, the current in the CW could be completely suppressed, forming an EIT-like window at a certain frequency. As the intensity of the pumping light increased, the conductivity of Si grew, and the bright and dark modes gradually became conductive. However, as the current direction of the bright and dark modes was antiparallel, they suppressed each other. As the conductivity

increased to a certain level, i.e., σ = 2000 S/m for instance, the coupling between bright and dark modes was almost completely suppressed. At this point, the current was limited around the CW area, while the LSP resonance as well as the EIT-like window disappeared, leaving only the LC resonance.
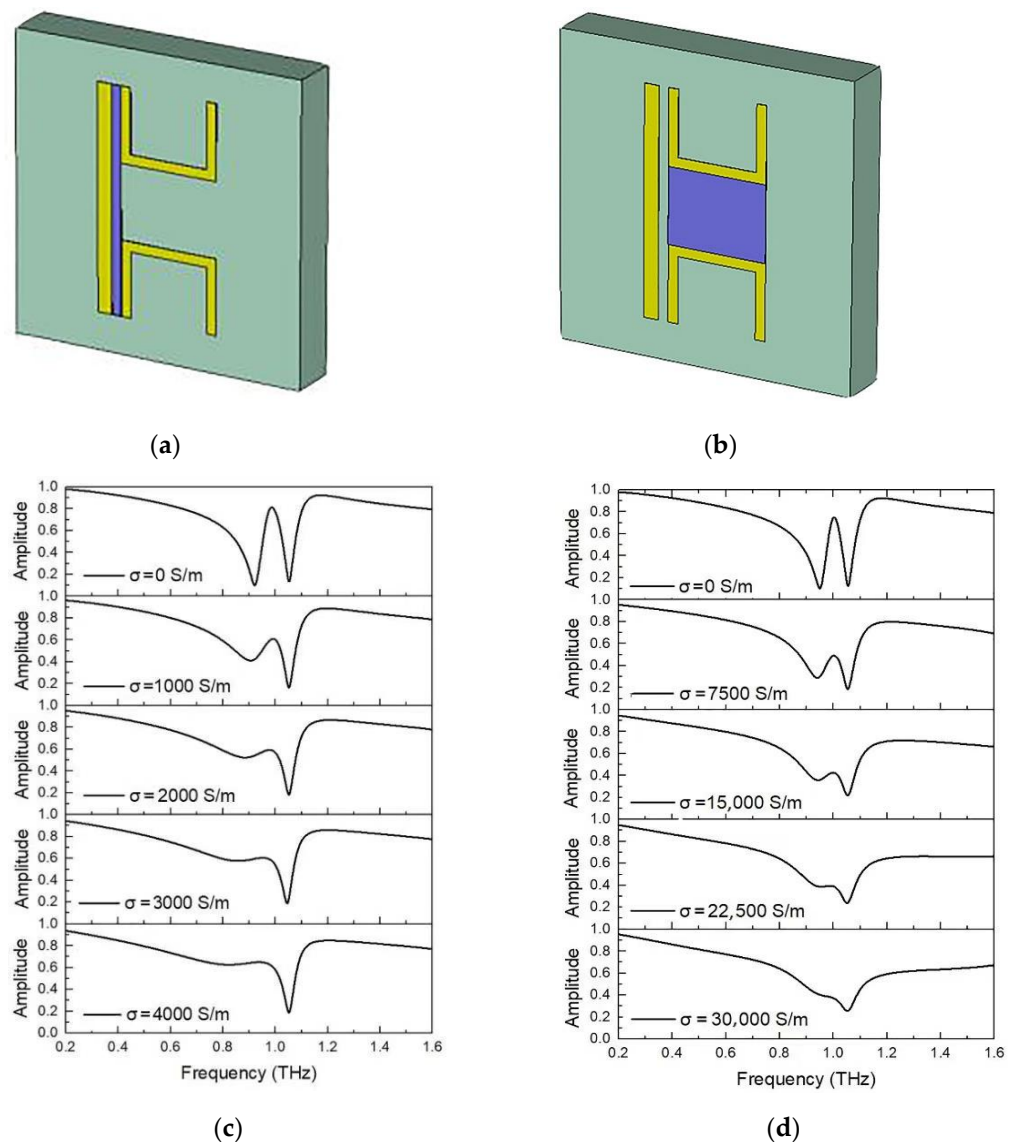

Figure 6. The effect of adding photosensitive Si into the metamaterial structure on the transmission characteristics. (**a**) Structure of buried photosensitive Si with different conductivity between CW and USRs; (**b**) Structure of buried photosensitive Si with different conductivity between USR pairs; (**c**) The transmission spectra buried with different conductivity photosensitive Si between CW and USRs. As the conductivity of Si battery increases, the LSP resonance disappears, so only LC resonance trough remains, while the EIT-like window disappears completely; (**d**) The transmission spectra of photosensitive Si buried with different conductivity between USR pairs. When the conductivity of the Si battery increases, the current will be limited around the CW, which cause the EIT-like window to completely disappear.

In addition, by burying photosensitive Si between the USR pairs, a similar modulation effect was found, see Figure 6b,d. In this structure, the two USRs were electrically isolated without introducing the pumping light, and the induced current flow around two separate USRs with the current in CW suppressed, forming an EIT-like window. The increasing of pumping intensity enhanced the conductivity of the Si, and therefore the conductivity

of the whole device. The currents in the USR structure tended to cancel each other as the direction of each was opposite. When the conductivity of Si became large enough (σ = 22,500 S/m), the current in USRs was suppressed and all the current was confined in the CW area, and in this case, no transparent window was found in the spectrum. It was found that the EIT-like transparent window could be actively modulated by changing the conductivity of the buried photosensitive Si structure. With the help of a proper pumping light intensity, the application of terahertz switch could be realized.

It can also be noticed that, the size of introduced Si structure can also play an important role of influencing the transparent window. Figure 7 shows the results of modulation effects by varying the effective length of photosensitive Si, L_{eff}, and the effective distance between two USRs, W_{eff}. In Figure 7a, the photosensitive Si is filled between the bright and dark modes and the conductivity is set to be 1000 S/m, it can be found that the larger effective length L_{eff} results in a stronger conductivity of the photosensitive Si, which shows significant influence on the EIT-like window of the metamaterial structure. Similarly, as shown in Figure 7b, with a setting conductivity of σ = 8000 S/m, the EIT-like window could be affected by varying the effective width of W_{eff}. As a result, by optimizing the structure size of the buried Si, the active modulation effect of the pumping light could be enhanced.

(**a**)   (**b**)
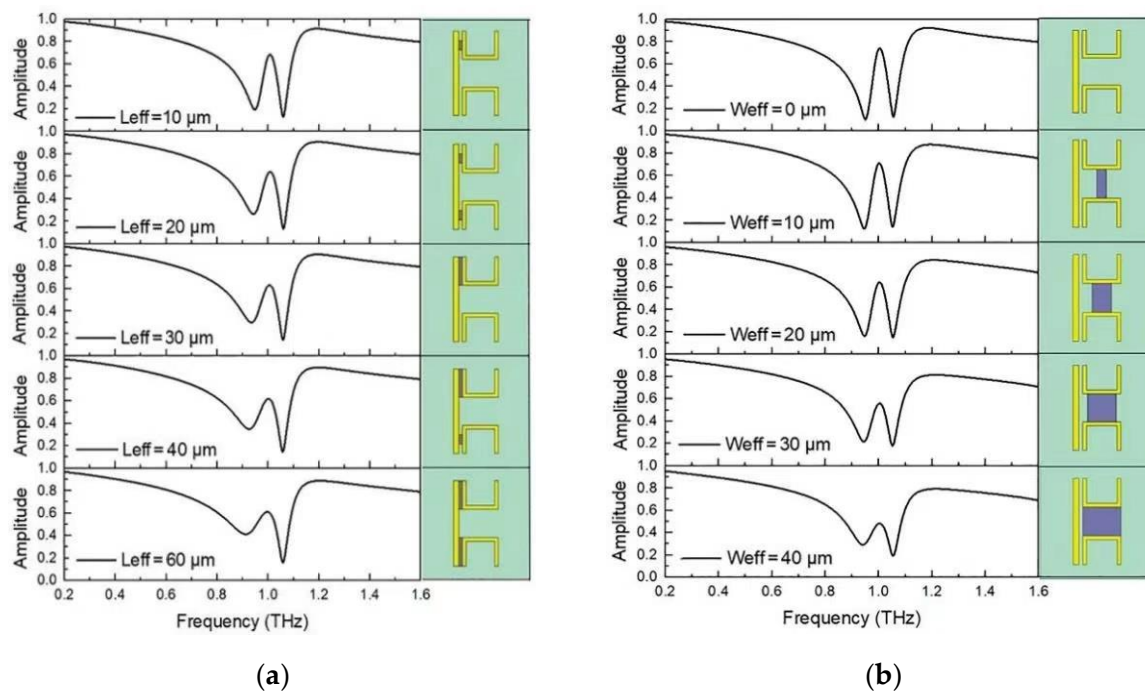
Figure 7. The influence of size parameters of photosensitive Si on transparent window. (**a**) The modulation effect of different effective length L_{eff} of photosensitive Si. As the L_{eff} is larger, the more obvious influence on the EIT-like window of the metamaterials; (**b**) The modulation effect of photosensitive Si with different effective width W_{eff}. With the increase of W_{eff}, the influence on the EIT-like window is greater.

In order to understand the active modulation effect of the photosensitive Si on the asymmetric structure, two types of Si positions, between the CW and USR as well as between the USRs were investigated. As shown in Figure 8a,c, the lengths of the two photosensitive Si structures were both set to be 30 μm. The widths were set as same as the coupling distance δ_{xup} and δ_{xdown}, which were 13 μm and 4 μm, respectively. In this case, the active modulation was due to the change of the conductivity of the photosensitive Si, leading to a change in the coupling effect between the bright and dark modes. The trend is consistent with that of the symmetric structure. However, as the conductivity of photosen-

sitive Si increased to 1000 S/m, the EIT-like window disappeared completely, which was only half of that required in the unilateral symmetric structure case (σ = 2000 S/m).
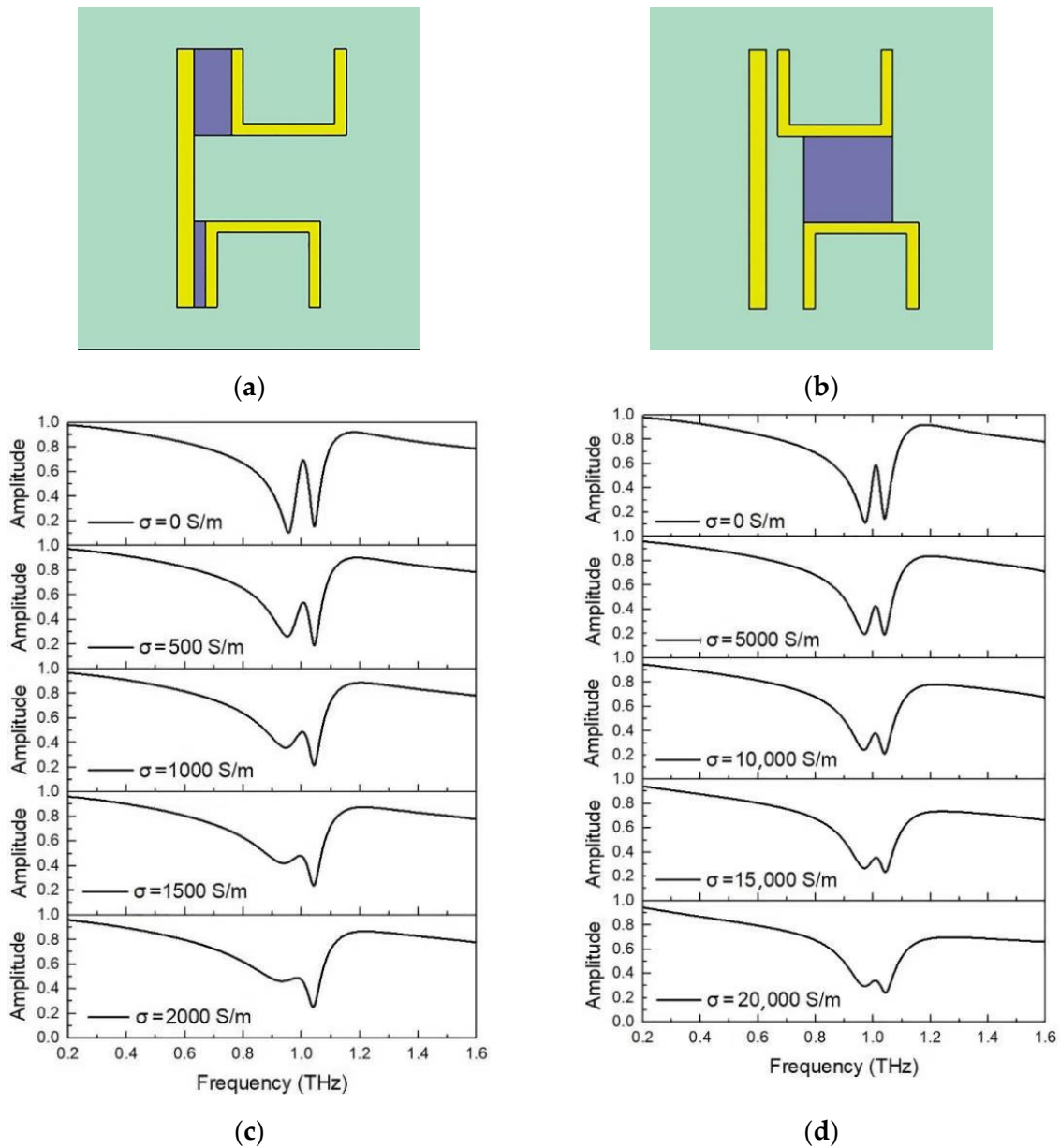

Figure 8. The effect of burying photosensitive Si between asymmetric metamaterials on the transparent window. (**a**) Structure of buried photosensitive Si with different conductivity between CW and USRs; (**b**) Structure of buried photosensitive Si between USR pairs; (**c**) The transmission spectra buried with different conductivity photosensitive Si between CW and USRs; (**d**) The transmission spectra of photosensitive Si buried between USR pairs.

The modulation effect of the buried Si between the asymmetric USR pairs on the transmission window is shown in Figure 8b,d. The width of photosensitive Si was set as 21 μm and the length was the same as the coupling distance δ_y, which was 9 μm. It can be found that the trend is also similar as the symmetric structure. However, as the conductivity of Si increased to 15,000 S/m, the current in the two USRs was completely suppressed, causing the EIT-like window to disappear completely. Compared with the unilateral symmetric structure in the same situation, the light intensity needed by the EIT-like window to disappear was smaller.

3.3. Refractive Index Sensing Characteristics of Metamaterial

It is known that the transmission spectra of terahertz metamaterials can drift with the change in the refractive index (RI) of the environment. In this work, three groups of metamaterials, the structure with only CW resonator, the metamaterials with unilateral symmetric structure, and metamaterials with unilateral asymmetric structure, were simulated. The quartz substrate and gold layer were used in the design of high sensitivity refractive index sensors for better stability and corrosion resistance properties. The sensing response came from the drift of LSP resonance peak/ EIT-like windows of different structures. A sensing dielectric layer of 3 μm thick was added with the change of refractive index from 1 to 2. It was observed that as the RI of the dielectric layer increased, both the resonance peak and the transparent window were red-shifted. In addition, the FWHM of the EIT-like window showed slight broadening while the resonance intensity was also weakened (see Figure 9a–c).
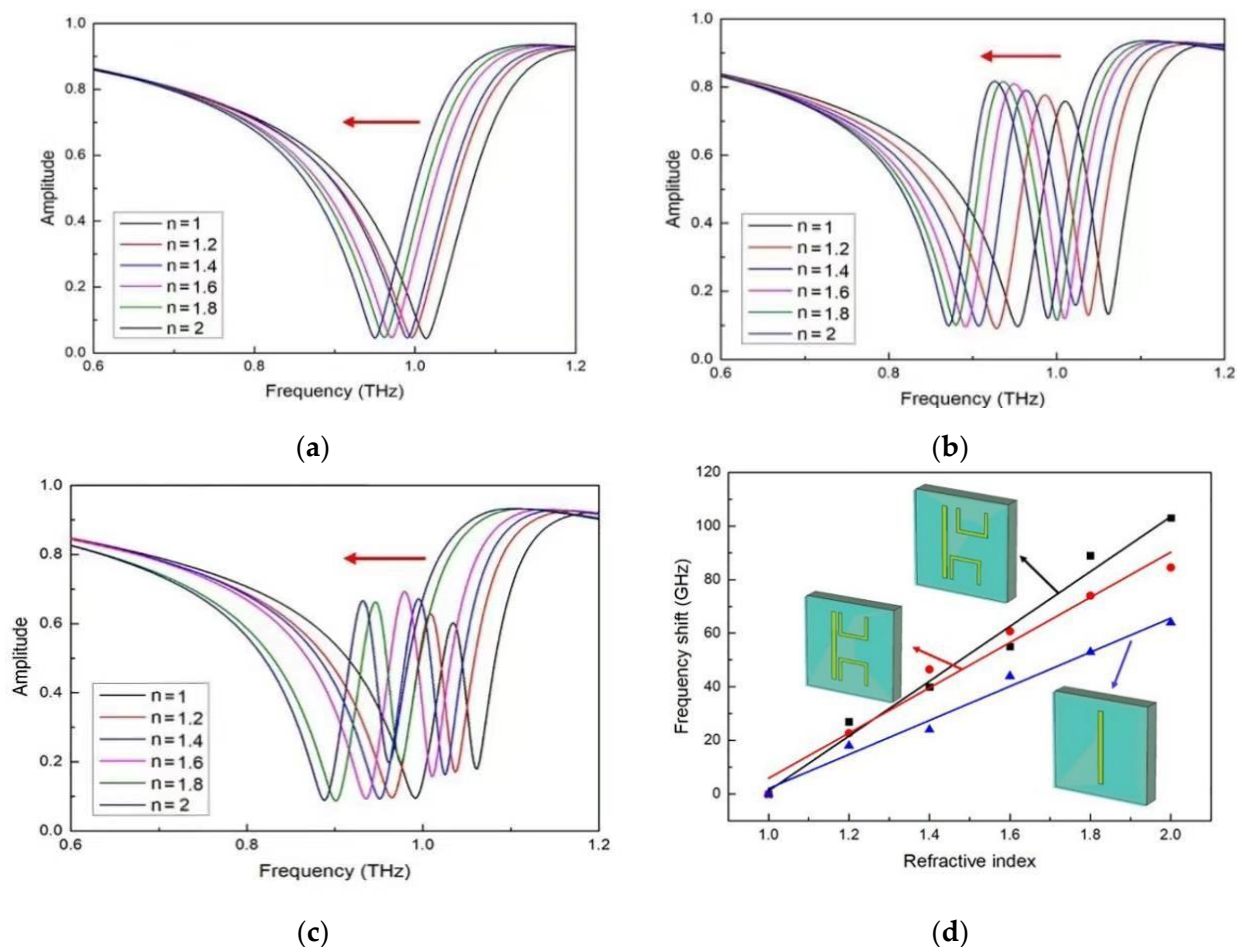
Figure 9. The influence of refractive index changes on the transmission spectra. (**a**) The transmission spectra of CW resonance peak varying with refractive index; (**b**) The transmission spectra of EIT-like window with unilateral symmetric structure varying with refractive index; (**c**) The transmission spectra of the EIT window with unilateral asymmetric structure varying with refractive index. With the increase of the refractive index of the dielectric layer, the resonance peak and the transparent window are red-shifted; (**d**) Linear fitting of the refractive index sensitivity against the drift of the peak frequency of three metamaterials.

The performance of the sensor was mainly characterized by several important parameters, including the refractive index sensitivity (S), Q-factor, and figure of merit (FOM). *S* is defined dip frequency shift per-refractive index unit: $S = \Delta f / \Delta n$. Q-factor is an important

parameter that determines the resonance, dispersion, and loss properties of EIT-like metamaterials, and reflects the resonance intensity and resolution of the sensor. Q is defined as: $Q = f/FWHM$. FWHM is the full width at half maximum of the resonance frequency. FOM obtained by dividing the sensitivity by FWHM used to characterize metamaterials sensing capabilities. FOM is described as: $Q = S/FWHM$. Figure 9d shows the fitting of the refractive index sensitivity of three metamaterials. All the three curves show linear relationship as the RI increases, indicating a promising potential for sensing applications. For the CW-only structure, it could achieve a refractive index sensitivity of 63.6 GHz/RIU. However, for the unilateral symmetric structure metamaterial, it could achieve sensitivity of 84.4 GHz/RIU, Q-factors of 33.67 and FOM of 2.81. The refractive index sensitivity, Q-factor, and FOM of the metamaterial with unilateral asymmetric structure were found to be 102.3 GHz/RIU, 51, 5.115, respectively. These results show that, compared with the resonant peak, the EIT-like window is more sensitive to the refractive index of the external environment, especially for the unilateral asymmetric material structure (102.3 GHz/RIU).

More specifically, the extracted results were compared with similar results reported in [10,11,17,28–30], as shown in Table 1. It can be found that the two metamaterial structure sensors proposed in this work showed broader bandwidth and good sensing properties. EIT-like terahertz metamaterial refractive index sensors have a wide range of promising applications in environmental, chemical, and biological diagnostics as well as other related fields.

Table 1. Performance comparison of various terahertz metamaterial sensors.

Structure	Bandwidth	Sensitivity	Q-Factor	FOM
	(THz)	(GHz/RIU)		
This work (unilateral symmetric)	0.6–1.2	84.4	33.67	2.8
This work (unilateral asymmetric)	0.6–1.2	102.3	51	5.115
Ref. [28]	0.15–0.85	54.18	–	–
Ref. [10]	0.6–1.2	102	20	2.99
Ref. [29]	1.05–1.17	49.3	65	–
Ref. [30]	0.4–1.0	180	0.22	–
Ref. [11]	0.8–1.6	163	7.036	2.67

4. Conclusions

In this paper, two kinds of metamaterial structures are proposed to realize an electromagnetic-like induced single transparent window, which are unilateral symmetric and unilateral asymmetric metamaterials. Various size parameters of the metamaterials were optimized to form EIT-like windows as well as modify them. By analyzing the distribution of electromagnetic field and surface current together with the transmission spectra of EIT-like window, the mechanism of EIT-like effect was investigated. In addition, the modulation effects of transparent windows of the two metamaterials were discussed, including both the passive modulation (changing the coupling distance) and active modulation (changing the conductivity of the photosensitive Si buried in the metamaterials). The tunability of EIT-like window under both modulation modes shows great potential for THz switches. Furthermore, the results show that the metamaterials of both structures can achieve high sensitivity refractive index response, up to 102.3 GHz/RIU, which can be applied for high sensitivity sensing purposes.

References

1. Harris, S.E. Electromagnetically induced transparency. *Phys. Today* **1997**, *50*, 36–42. [CrossRef]
2. Hau, L.V.; Harris, S.E.; Dutton, Z.; Behroozi, C.H. Light speed reduction to 17 metres per second in an ultracold atomic gas. *Nature* **1999**, *397*, 594–598. [CrossRef]
3. Sultana, J.; Islam, M.S.; Ahmed, K.; Dinovitser, A.; Ng, B.W.H.; Abbott, D. Terahertz detection of alcohol using a photonic crystal fiber sensor. *Appl. Opt.* **2018**, *57*, 2426–2433. [CrossRef] [PubMed]
4. Zhang, L.; Tassin, P.; Koschny, T.; Kurter, C.; Anlage, S.M.; Soukoulis, C.M. Large group delay in a microwave metamaterial analog of electromagnetically induced transparency. *Appl. Phys. Lett.* **2010**, *97*, 241904. [CrossRef]
5. Yin, X.G.; Feng, T.H.; Yip, S.; Liang, Z.X.; Hui, A.; Ho, J.C.; Li, J.S. Tailoring electromagnetically induced transparency for terahertz metamaterials: From diatomic to triatomic structural molecules. *Appl. Phys. Lett.* **2013**, *103*, 021115. [CrossRef]
6. Liu, M.; Tian, Z.; Zhang, X.Q.; Gu, J.Q.; Ouyang, C.M.; Han, J.G.; Zhang, W.L. Tailoring the plasmon-induced transparency resonances in terahertz metamaterials. *Opt. Express* **2017**, *25*, 19844–19855. [CrossRef] [PubMed]
7. Singh, R.; Rockstuhl, C.; Menzel, C.; Meyrath, T.P.; He, M.X.; Giessen, H.; Lederer, F.; Zhang, W.L. Spiral-type terahertz antennas and the manifestation of the Mushiake principle. *Opt. Express* **2009**, *17*, 9971–9980. [CrossRef]
8. Schurig, D.; Mock, J.J.; Justice, B.J.; Cummer, S.A.; Pendry, J.B.; Starr, A.F.; Smith, D.R. Metamaterial electromagnetic cloak at microwave frequencies. *Science* **2006**, *314*, 977–980. [CrossRef]
9. Gu, J.Q.; Han, J.G.; Lu, X.C.; Singh, R.; Tian, Z.; Xing, Q.R.; Zhang, W.L. A close-ring pair terahertz metamaterial resonating at normal incidence. *Opt. Express* **2009**, *17*, 20307–20312. [CrossRef]
10. Cao, P.F.; Li, C.C.; Li, Y.; Wu, Y.Y.; Chen, X.Y.; Wu, T.; Zhang, X.Q.; Yuan, M.R.; Wang, Z.L. Electromagnetically Induced Transparency-Like Approach Based on Terahertz Metamaterials for Ultrasensitive Refractive Index Sensors. *IEEE Sens. J.* **2022**, *22*, 2110–2118. [CrossRef]
11. Wang, W.; Yan, F.P.; Tan, S.Y.; Zhou, H.; Hou, Y.F. Ultrasensitive terahertz metamaterial sensor based on vertical split ring resonators. *Photonics Res.* **2017**, *5*, 571–577. [CrossRef]
12. Papasimakis, N.; Fu, Y.H.; Fedotov, V.A.; Prosvirnin, S.L.; Tsai, D.P.; Zheludev, N.I. Metamaterial with polarization and direction insensitive resonant transmission response mimicking electromagnetically induced transparency. *Appl. Phys. Lett.* **2009**, *94*, 211902. [CrossRef]
13. Papasimakis, N.; Fedotov, V.A.; Zheludev, N.I.; Prosvirnin, S.L. Metamaterial Analog of Electromagnetically Induced Transparency. *Phys. Rev. Lett.* **2008**, *101*, 253903. [CrossRef]
14. Liu, N.; Weiss, T.; Mesch, M.; Langguth, L.; Eigenthaler, U.; Hirscher, M.; Sonnichsen, C.; Giessen, H. Planar Metamaterial Analogue of Electromagnetically Induced Transparency for Plasmonic Sensing. *Nano Lett.* **2010**, *10*, 1103–1107. [CrossRef] [PubMed]
15. Zhang, S.; Genov, D.A.; Wang, Y.; Liu, M.; Zhang, X. Plasmon-induced transparency in metamaterials. *Phys. Rev. Lett.* **2008**, *101*, 047401. [CrossRef]
16. Zhu, Z.H.; Yang, X.; Gu, J.Q.; Jiang, J.; Yue, W.S.; Tian, Z.; Tonouchi, M.; Han, J.G.; Zhang, W.L. Broadband plasmon induced transparency in terahertz metamaterials. *Nanotechnology* **2013**, *24*, 214003. [CrossRef] [PubMed]
17. Pan, W.; Yan, Y.J.; Ma, Y.; Shen, D.J. A terahertz metamaterial based on electromagnetically induced transparency effect and its sensing performance. *Opt. Commun.* **2019**, *431*, 115–119. [CrossRef]
18. Xia, S.X.; Zhai, X.; Wang, L.L.; Sun, B.; Liu, J.Q.; Wen, S.C. Dynamically tunable plasmonically induced transparency in sinusoidally curved and planar graphene layers. *Opt. Express* **2016**, *24*, 17886–17899. [CrossRef]
19. Shu, C.; Chen, Q.G.; Mei, J.S.; Yin, J.H. Analogue of tunable electromagnetically induced transparency in terahertz metal-graphene metamaterial. *Mater. Res. Express* **2019**, *6*, 055808. [CrossRef]
20. Patel, S.K.; Surve, J.; Jadeja, R.; Katkar, V.; Parmar, J.; Ahmed, K. Ultra-Wideband, Polarization-Independent, Wide-Angle Multilayer Swastika-Shaped Metamaterial Solar Energy Absorber with Absorption Prediction using Machine Learning. *Adv. Theor. Simul.* **2022**, 2100604. [CrossRef]
21. Shen, S.M.; Liu, Y.L.; Liu, W.Q.; Tan, Q.L.; Xiong, J.J.; Zhang, W.D. Tunable electromagnetically induced reflection with a high Q factor in complementary Dirac semimetal metamaterials. *Mater. Res. Express* **2018**, *5*, 125804. [CrossRef]

22. Liu, X.J.; Gu, J.Q.; Singh, R.; Ma, Y.F.; Zhu, J.; Tian, Z.; He, M.X.; Han, J.G.; Zhang, W.L. Electromagnetically induced transparency in terahertz plasmonic metamaterials via dual excitation pathways of the dark mode. *Appl. Phys. Lett.* **2012**, *100*, 131101.

23. Li, Z.Y.; Ma, Y.F.; Huang, R.; Singh, R.J.; Gu, J.Q.; Tian, Z.; Han, J.G.; Zhang, W.L. Manipulating the plasmon-induced transparency in terahertz metamaterials. *Opt. Express* **2011**, *19*, 8912–8919. [CrossRef] [PubMed]

24. Jiang, J.X.; Cui, J.F.; Fang, R.Q.; Wu, F.M.; Yang, Y.Q. Tunable Electromagnetically Induced Transparency in Asymmetric Graphene-Based Metamaterial at Terahertz Region. *Integr. Ferroelectr.* **2020**, *212*, 1–8. [CrossRef]

25. Chiam, S.Y.; Singh, R.; Rockstuhl, C.; Lederer, F.; Zhang, W.L.; Bettiol, A.A. Analogue of electromagnetically induced transparency in a terahertz metamaterial. *Phys. Rev. B* **2009**, *80*, 153103. [CrossRef]

26. Yahiaoui, R.; Burrow, J.A.; Mekonen, S.M.; Sarangan, A.; Mathews, J.; Agha, I.; Searles, T.A. Electromagnetically induced transparency control in terahertz metasurfaces based on bright-bright mode coupling. *Phys. Rev. B* **2018**, *97*, 155403. [CrossRef]

27. Liu, N.; Langguth, L.; Weiss, T.; Kastel, J.; Fleischhauer, M.; Pfau, T.; Giessen, H. Plasmonic analogue of electromagnetically induced transparency at the Drude damping limit. *Nat. Mater.* **2009**, *8*, 758–762. [CrossRef]

28. Yahiaoui, R.; Tan, S.Y.; Cong, L.Q.; Singh, R.; Yan, F.P.; Zhang, W.L. Multispectral terahertz sensing with highly flexible ultrathin metamaterial absorber. *J. Appl. Phys.* **2015**, *118*, 083103. [CrossRef]

29. Singh, R.; Cao, W.; Al-Naib, I.; Cong, L.Q.; Withayachumnankul, W.; Zhang, W.L. Ultrasensitive terahertz sensing with high-Q Fano resonances in metasurfaces. *Appl. Phys. Lett.* **2014**, *105*, 171101. [CrossRef]

30. Rodriguez-Ulibarri, P.; Kuznetsov, S.A.; Beruete, M. Wide angle terahertz sensing with a cross-dipole frequency selective surface. *Appl. Phys. Lett.* **2016**, *108*, 111104. [CrossRef]